Nuclear Physics B252 (1985) 261-276
North-Holland, Amsterdam

EXPERIMENTAL LIMITS ON MONOPOLE CATALYSIS, $N\bar{N}$ OSCILLATIONS, AND NUCLEON LIFETIMES *

Presented by
James L. STONE, Randall Laboratory of Physics, The University of Michigan, Ann Arbor, Michigan 48109, USA

H.S. PARK[2], G. BLEWITT[4], B.G. CORTEZ[4], G.W. FOSTER[2], W. GAJEWSKI[1], T.J. HAINES[1], D. KIELCZEWSKA[1,8], J.M. LOSECCO[4], R.M. BIONTA[2], C.B. BRATTON[5], D. CASPER[2], P. CHRYSICOPOULOU[2], R. CLAUS[2], S. ERREDE[2], K.S. GANEZER[1], M. GOLDHABER[3], T.W. JONES[7], W.R. KROPP[1], J.G. LEARNED[6], E. LEHMANN[4], F. REINES[1], J. SCHULTZ[1], S. SEIDEL[2], E. SHUMARD[2], D. SINCLAIR[2], H.W. SOBEL[1], J.L. STONE[2], L.R. SULAK[2], R. SVOBODA[6], J.C. VAN DER VELDE[2] and C. WUEST[1]

[1]The University of California at Irvine, Irvine, California 92717, USA

[2]The University of Michigan, Ann Arbor, Michigan 48109, USA

[3]Brookhaven National Laboratory, Upton, New York 11973, USA

[4]California Institute of Technology, Pasadena, California 91125, USA

[5]Cleveland State University, Cleveland, Ohio 44115, USA

[6]The University of Hawaii, Honolulu, Hawaii 96822, USA

[7]University College, London WC1E 6BT, UK

[8]Warsaw University, Warsaw PL-00-681, Poland

*Work supported by the U.S. Department of Energy.

A 3300 metric tonne fiducial mass ring-imaging water Cherenkov detector has been used to search for experimental evidence of nucleon decay, monopole catalysis, and $n \to \bar{n}$ transitions in oxygen. No unambiguous events have been observed for any of these processes. We report 90% C.L. lower limits on the nucleon lifetime for 32 possible decay modes. In addition, limits on the cosmic monopole flux based on the non-observation of a time sequence of multiple catalyzed nucleon decays are reported. Also reported is a bound lifetime lower limit for $n\bar{n}$ oscillations in oxygen nuclei.

THE IMB DETECTOR

The Irvine-Michigan-Brookhaven (IMB) nucleon lifetime detector is located at a depth of 1570 meters of water equivalent (mwe) in the Morton-Thiokol salt mine near Fairport Harbor, Ohio. The detector consists of a large rectangular volume (17 m × 18 m × 23 m) of ultra-purified water viewed from its six faces by 2048 hemispherical photomultiplier tubes (PMTs), each of 12.5 cm diameter. The PMTs are spaced on a 1 m rectangular lattice. The total sensitive volume of the detector is 8000 metric tonnes. A fiducial volume of 3300 metric tonnes (2.0×10^{33} nucleons) is defined by the region inset 2m from the planes of the PMTs.

A relativistic charged particle traversing the detector produces a cone of Cherenkov light with an opening half angle of 41° relative to its direction of motion. The particle continues to emit Cherenkov light until its velocity falls below 0.75 c. The particles $\mu^{\pm}$, $\pi^{\pm}$, and $K^{\pm}$ are visible above total energy thresholds of 160, 215, and 750 MeV respectively. In contrast, the particles $e^{\pm}$, γ, and π° produce electromagnetic showers in which essentially all their energy is deposited in the detector. The total light yield of an event, E_C, is obtained after correction for light attenuation in water, PMT angular response, pulse height non-linearity, and other systematic effects. The absolute scale of E_C is normalized by studying throughgoing muons which emit a known amount of Cherenkov light.

The readout electronics records for each PMT the time of arrival (T1) and the amount (Q) of Cherenkov light at that tube. The T1 time scale spans a period of 512 ns with 1 ns least count. The detector is triggered whenever ≥3 PMTs in a group of 8 × 8 tubes fire within 50 ns and any 2 or more groups of tubes fire within 150 ns. A second unbiased trigger requires ≥ 12 PMTs to fire within 50 ns. These trigger requirements correspond to energy thresholds of 25 and 50 MeV respectively. Immediately following a trigger on the T1 time scale, the electronics activates for each PMT a second time scale (T2) extending to 7.5 μs with 15 ns least count. This T2 time scale enables the detection of $\mu \to e\nu\bar{\nu}$ decays.

A muon decay electron is identified by a coincidence of 5 or more PMTs in any 60 ns window on the T2 time scale. Using a sample of entering stopping tracks, the efficiency for μ^+ detection is measured to be ~ 62%. About 30% of the neutrino events are expected to have an identified μ-decay.

Two distinguishing characteristics of this detector are its large sensitive mass and its ability to determine unambiguously the sense of track direction. The uniform sensitivity of the active medium makes the energy resolution of the detector relatively independent of the fluctuations of electromagnetic shower development and Fermi motion of the decaying proton. Performance checks of the detector operation were made by measuring the muon angular distribution, stopping muon rate, and muon lifetime. These measurements are consistent with accepted values. An underwater photograph of a portion of the IMB detector is shown in Fig. 1.

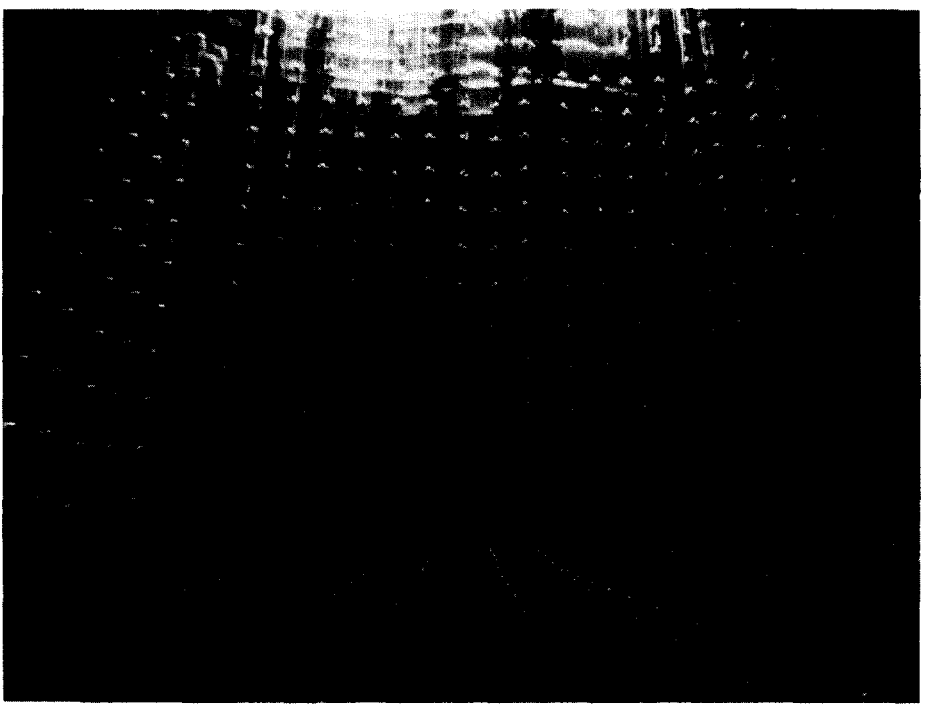

Fig. 1 Underwater photograph of the IMB nucleon decay experiment. The photo is a time exposure taken at a depth of ~ 20 m at the bottom of the water containment vessel. The photomultiplier tubes are located on all six sides of the water tank and are spaced 1 m apart. The extreme clarity of the ultrapure water is apparent. (Photo by Karl Luttrell)

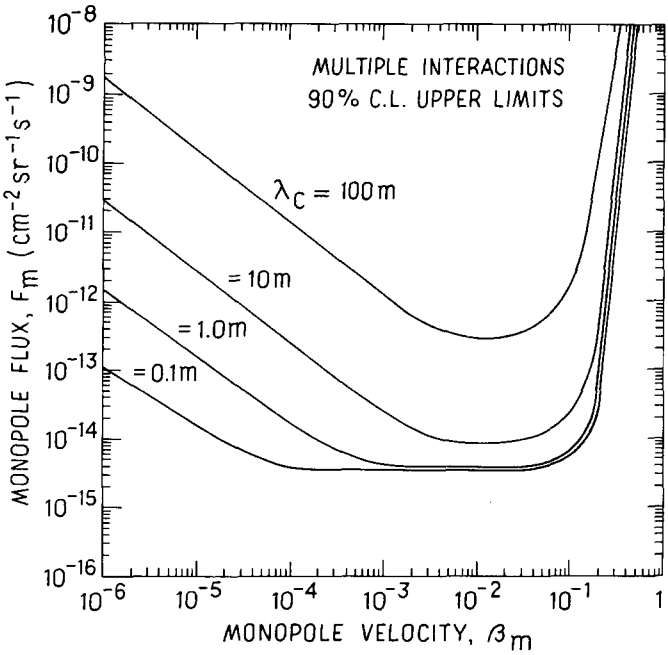

Fig. 2 The IMB 90% C.L. monopole flux limits for multiple (> 2) monopole catalysis of nucleon decay interactions. Contours are drawn for constant interaction lengths, λ_c, as indicated.

If the catalysis interaction length, λ_c, is larger than the mean path length, <L>, through the detector, then only single catalysis interactions are likely to occur in the detector. Due to the kinematics of the catalysis reaction[9], single interactions may be indistinguishable from events due to atmospheric neutrino interactions.

In an independent search for spontaneous nucleon decay, the IMB experiment has observed 169 events with energies below twice the nucleon rest mass in 204 days of analyzed data. The rate and energy distribution of these events are consistent with atmospheric neutrino interactions. However, if one assumes that they are due to monopole catalysis, then a conservative 90% C.L. upper limit on the monopole flux is obtained which is independent of the monopole velocity. In Fig. 3 the monopole flux limit derived by this analysis is plotted as a function the interaction length. Since the number of single interactions occurring in the detector are constant with time, this limit will not improve with additional detector livetime.

MONOPOLE CATALYSIS OF NUCLEON DECAY

One of the more exciting ideas to emerge from GUTs is the suggestion by Callan[1], Rubakov[2], and Wilczek[3] that superheavy magnetic monopoles may catalyze nucleon decay via the interaction

$$M + N \rightarrow M' + e^+ + \text{meson(s)}, \text{ where } N = n \text{ or } p.$$

The cross section for this process is expected to be of the order typical for strong interactions, i.e., $\sigma_c \sim 0.1 - 10$ mb, for monopoles in the velocity range $10^{-4} < \beta_m < 10^{-2}$. Hence, the possibility exists that large nucleon decay detectors now on the air could detect a time sequence of multiple (>2) catalyzed nucleon decays with essentially no background. Such an observation would be a tremendous boost for GUTs in that it would represent the simultaneous discovery of monopoles and nucleon decay.

Data have been reported from 5 nucleon decay experiments: Kolar Gold Field[4], Soudan I[5], Mont Blanc[6], Kamioka[7], and IMB[8]. None of the experiments has observed catalyzed decays. Summaries of the detector properties and the monopole flux limits derived from these experiments are given in Tables I and II respectively. A comprehensive review of terrestrial experimental searches for monopole catalysis of nucleon decay can be found in Ref. 9 .

The IMB experiment utilizes the 2 time scales associated with the detector electronics to search for multiple catalyzed decays. T1 time scale extends to 0.5 μs and a T2 scale keeps the detector live for an additional 7.5 μs. Following a trigger on the T1 scale, the T2 scale is activated. The IMB monopole trigger requires at least one event with > 30 PMTs in coincidence on the T1 time scale and at least one additional event with > 50 PMTs within any 300 ns window on the T2 time scale. The measured event rate is 4.6 ± 0.3 coincidences/day. This is consistent with the expected rate of 4.7 events/day due to random two-fold coincidences from the 2.7 muons/second which pass through the detector. All coincident events were scanned by physicists and rejected as entering random cosmic ray muons.

With no observed events, we report 90% C.L. upper limits on the monopole flux based on 300 days of analyzed data for constant values of the monopole catalysis interaction mean free path, λ_c. These results are plotted as a function of monopole velocity, β_m, in Fig. 2. The flux limits have decreased sensitivity in the high velocity region because of the increased probability of all catalysis interactions occurring only on the T1 time scale. In the low velocity region, the decreased sensitivity is due to the increased probability of the second catalysis interaction occurring after the end of the T2 time scale. It should be noted that since the flux limits are a function of both β_m and λ_c, the contours in Fig. 2 are slices through a surface in F_m-β_m-λ_c.

Table I. Physical Properties of the Nucleon Decay Detectors.

	(units)	Soudan I	KGF	Mont Blanc	Kamioka	IMB
Depth	(hg/cm^2)	1800	7000	5200	2700	1500
Detector Material		Taconite Cement	Iron	Iron	H_2O	H_2O
Ave. Density	(gm/cm^3)	1.9	1.5	3.5	1.0	1.0
Total Mass	(tonnes)	31	140	150	3000	8000
Fiducial	(tonnes)	16	100	100	1000	3300
Dimensions	(m)	3×3×2	4×4×6	$(3.5)^3$	15.5ϕ×16	23×17×18
Eff. Area	(m^2)	10	32	18	220	550
Ave. Path Length	(m)	1.7	3.1	2.3	10.3	12.8
Electronics Live Time	(sec)	6.5	7.0	5.0	88	8.0

Table II. Summary of Monopole Flux Limits derived from the Nucleon Decay Experiments

Detector	Live Time (days)	Interaction Length, λc (meters)	Velocity Range (β)	Monopole Flux Limits ($cm^{-2}sr^{-1}s^{-1}$) ≡ 1 Interaction	≥ 2 Interactions
KGF	561	λ_c=4m		2×10^{-13}	
	561	σ_c>10mb	$\beta_m>10^{-3}$		2×10^{-14}
Soudan I	285	$10^{-2}<\sigma_o<10^{2}$	$\beta_m>10^{-3}$		1.5×10^{-13}
Mont Blanc	317	$\lambda_c\approx4$m	$\beta_m>10^{-4}$	6.1×10^{-13}	
	317	λ_c<1m	$\beta_m>10^{-4}$		2.3×10^{-14}
Kamioka	135	λ_c<1.7m	$10^{-4}<\beta_m<10^{-3}$		7.6×10^{-14}
	135	λ_c<17m	$10^{-5}<\beta_m<10^{-3}$		6.4×10^{-15}
IMB	200	$\lambda_c\approx16.7$m		1.7×10^{-12}	
	300	λ_c<1.0m	$5\times10^{-3}<\beta_m\times10^{-2}$		2.4×10^{-15}
	300	λ_c<0.1m	$10^{-3}<\beta_m<10^{-1}$		2.1×10^{-15}

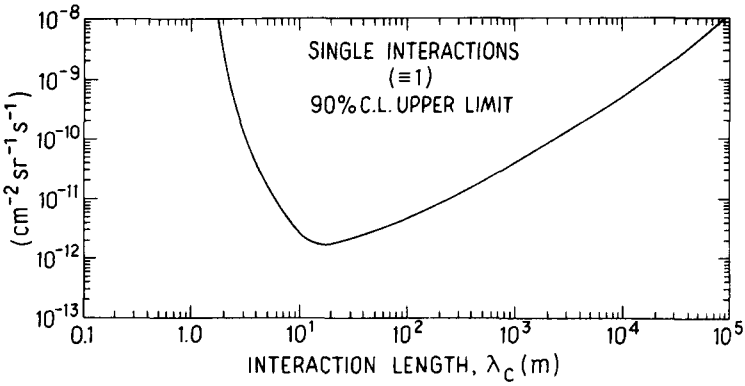

Fig. 3 The IMB 90% C.L. flux limit for single monopole catalysis of nucleon decay interactions. This conservative limit assumes all observed events are due to catalysis.

NEUTRON-ANTINEUTRON OSCILLATIONS IN OXYGEN

Recent grand unification theories allow the possibility of both nucleon decay ($\Delta B=1$) and neutron-antineutron transition ($\Delta B=2$) processes. However, some schemes, eg. SU(5), predict nucleon decay but forbid n to $\bar{n}$ transitions. A review of the phenomenology of $n\bar{n}$ oscillations in nuclei can be found in Ref. 10.

The IMB experiment has searched for $n\bar{n}$ oscillations in oxygen nuclei. We use the fact that in general several pions will be created when the $\bar{n}$ annihilates inside a nucleus. The pions from the annihilation must be propagated through the nucleus and through the water of the detector. A detailed description of this analysis can be found in Ref. 11. In general, these events will show up as wide-angle or isotropic events in the IMB detector. A variable "isotropy angle" is defined to distinguish these events from neutrino background events which produce light predominantly in one hemisphere.

In Fig. 4 the event energy is plotted versus isotropy angle for 109 data events collected during 132 days of detector livetime. The event energy, E_C, represents a lower limit on the energy released in the interaction since it is based on the assumption that all particles are showering and massless. The true energy requires the addition of ~ 250 MeV for each charged pion or muon in the event. If the "isotropy angle" and event energy are required to be greater than 20° and 500 MeV respectively, then 50% of the simulated $n\bar{n}$ events successfully pass through the analysis chain. Three data events fall within the cuts. Monte Carlo simulations of the expected background from atmospheric

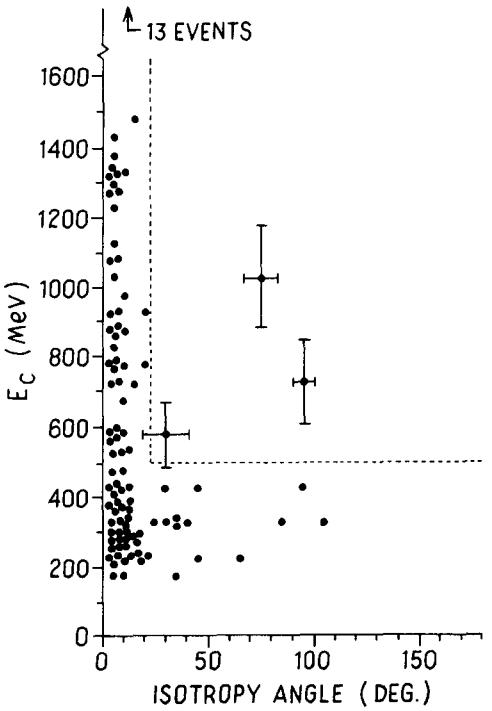

Fig. 4 Cherenkov energy vs. isotropy angle for 109 contained events. The horizontal error bars which are typical indicate the uncertainty in angle due to the uncertainty in the vertex position. Vertical error bars represent our ±15% (systematic plus statistical) uncertainty in in energy. The dotted lines indicate the region of acceptance.

neutrino interactions are consistent with the data plotted in Fig. 4. However, until this background is better understood, no subtraction is made from the three events. Thus, a 90% C.L. lower limit is obtained using 6.7 events and a detection efficiency of 50%,

$$\tau\,(n \to \bar{n}) > \frac{(8.9 \times 10^{32}\ \text{neutrons})\ (0.362\ \text{yr.})\ (0.55 \times 0.9\ \text{efficiency})}{6.7\ \text{events}\ (90\%\ \text{C.L.})}$$

$$= 2.4 \times 10^{31}\text{years}$$

The calculations of Dover, Gal, and Richard[12] show that in oxygen a bound lifetime > 10^{31} years leads to a limit of $\tau\,(n \to \bar{n}) > 5.7 \times 10^{7}$ seconds on the free space oscillation time. Using this result, the IMB bound lifetime limit translates to a lower limit on the free-neutron oscillation time of 8.8×10^{7} seconds.

NUCLEON LIFETIME LIMITS FOR TWO AND THREE BODY DECAY MODES[13]

We present results from the IMB experiment for 32 nucleon decay modes based on 204 days of detector livetime. Within this time, ~ 5×10^7 triggers have been recorded, mostly due to cosmic ray muons. A few percent of the triggers are multiple muon events or muons stopping in the detector volume. Upward going muons resulting from neutrino interactions in the rock below the detector are observed at a rate of ~ 1 event/week. Neutrino interactions contained within the fiducial volume are observed at a rate of $\lesssim$ 1 event/day.

The goal of the data analysis chain is to identify and reconstruct all events contained within the detector fiducial volume in the energy range $150 < E_C < 2000$ MeV, where E_C is the observed Cherenkov energy. These events will consist of neutrino interactions, possible nucleon decays, possible $n\bar{n}$ transitions, and perhaps other new physics.

Computer simulations of the IMB detector response show that neutrino interactions inside this energy range are saved with an efficiency > 90% at the higher energies and > 70% at lower energies. Nucleon decay events such as $p \to e^+\pi^\circ$ are saved with > 90% efficiency. Two independent analyses are carried out at the University of Michigan and at the University of California at Irvine. The overlap of the two analyses is consistent with the above efficiencies.

In 204 days of analyzed data, 169 events have been observed which originate in the detector fiducial volume and fall in the energy range $150 < E_C < 2000$ MeV. Some of the events have clear and reconstructable tracks, while others have no obviously distinguishable track. Other events may have one or more distinguishable tracks plus a significant number of hit PMTs which cannot be associated with a track. The various nucleon decay modes will produce PMT hit patterns which vary in topology and the number of distinguishable tracks.

For nucleon decay modes like $e^+\pi^\circ$, $e^+\pi^-$, $\mu^+\pi^\circ$, $\mu^+\pi^-$, two clearly separated tracks with an included angle > 150° are expected. For this class of events, there are three constraints used to reject neutrino induced background events, viz. (1) total energy, (2) included angle, and (3) energy sharing between the two tracks.

For final states like $\mu^+(K^\circ \to 2\pi^\circ)$, $\nu(K^\circ \to 2\pi^\circ)$, $\mu^+(\eta^\circ \to 3\pi^\circ, \gamma\gamma)$, and $n \to \bar{n}$, significant amounts of Cherenkov light fall outside of a single hemisphere. This class of events is characterized by three parameters: (1) the the observed Cherenkov energy, E_C, (2) the number of $\mu \to e\nu\bar{\nu}$ decays; and (3) the anisotropy, A. The variable, A, is defined as the magnitude of the sum of the unit vectors from the reconstructed vertex to each hit PMT and will

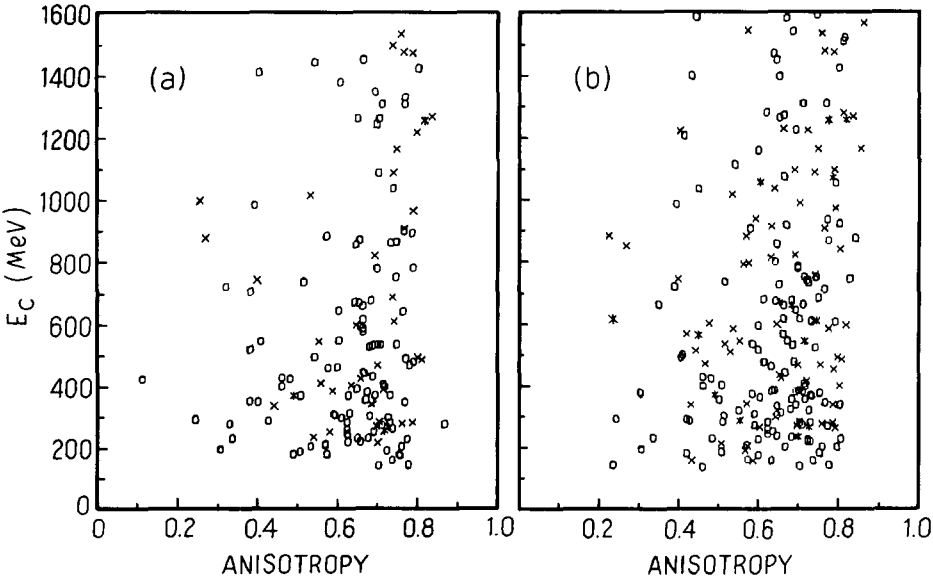

Fig. 5 (a) E_C vs. A for the 169 contained events from 204 live days of data. Events with 0, 1, and 2 identified $\mu \rightarrow e$ decays are indicated by 'o', 'x', and '*', respectively. (b) E_C vs. A for a simulation of 204 days of atmospheric ν interactions.

have values in the range $0 \leq A \leq 1$. Events which consist of a single non-showering track (eg. muon) will have $A \simeq 0.75$, which is the cosine of the Cherenkov half angle (41°). Events which have an isotropic pattern of hit PMTs are wide angle or multibody decays. These latter events are characteristic of most nucleon decays and typically will have values of $A \leq 0.5$. Fig. 5a shows the distribution of E_C vs. A for the 169 events observed in 204 days of analyzed data.

Each individual nucleon decay mode is studied by Monte Carlo simulation which includes Fermi motion and nuclear interactions of mesons in both oxygen and water (eg. pion and kaon scattering, absorption and charge exchange as well as K_L° interactions). The generated Monte Carlo events are plotted as E_C vs. A in Fig. 5b. For each mode, cuts are chosen for E_C, A, and number of muon decays to give the best signal-to-background for that mode. For simplicity, rectangular cuts in E_C vs. A are chosen. The detection efficiency for a given mode is determined by the fraction of the simulated events falling within the cuts. For modes where physicist scanning may be involved, the simulated events are scanned using a color-graphics system.

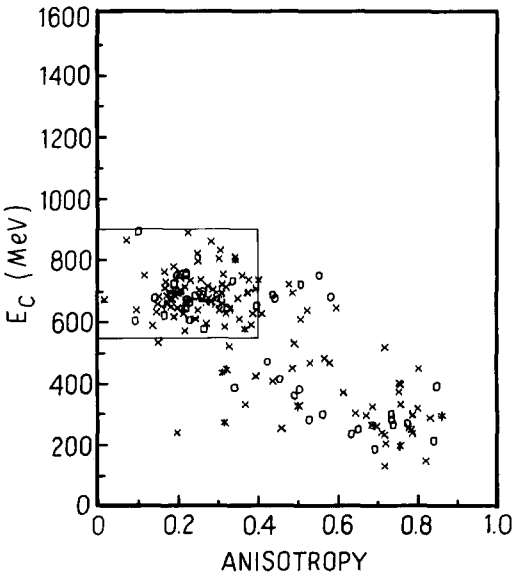

Fig. 6 E_C vs. A for a representative simulated nucleon decay mode, $p \to \mu^+\pi^\circ$. The square box indicates the region in which candidates are accepted for this mode.

This method determines the scanning efficiencies. In addition to the E_C vs. A cuts, some modes can be further constrained by topological information such as number of distinguishable tracks, included angle, and energy sharing among tracks. As an example, Fig. 6 shows a plot of the generated nucleon decay events and cuts chosen for the mode $p \to \mu^+\pi^\circ$.

The neutrino induced background was simulated using data from Gargamelle freon bubble chamber. Gargamelle events which fall in the acceptance region for proton decay have been scanned to remove contamination due to entering tracks or interactions in the chamber walls. The reconstructed particle types and momenta of the "cleaned up" Gargamelle data were used as input to the IMB simulation program. The generated events were weighted by the atmospheric neutrino spectrum and put through the full data analysis chain. This technique accounts for complicated nuclear effects which influence the topology and particle multiplicity distributions for neutrino interactions. Although this method is not perfect in that freon is not water, we believe that within the quoted systematic errors, it is a more realistic background estimate than could be gleaned from a first-principles Monte Carlo simulation. The number of background events for each mode listed in Table III below was

Table III - IMB Nucleon Decay Partial Lifetime Limits

1	2	3	4	5	6	7	8	9	10
Mode	Requirements				Effic. with Nuclear Corr.	Effic. without Nuclear Corr.	Candi-dates Observed	No. of Bkgnd. Est. -50%, +100%	Limit on τ/B $\times 10^{31}$ yr 90% C.L.
	E_c (Mev)	A	#μ	Back to Back					
$p \to e^+\gamma$	750-1100	< 0.3	0	0	0.66	0.66	0	0.1	18.
$p \to e^+\pi^\circ$	750-1100	< 0.3	0	0	0.46	0.75	0	0.1	12.
$p \to e^+K^\circ$	300-500	< 0.5	1		0.12	0.12	i	2	
	750-1100	< 0.3	0		0.14	0.14	0	0.2	4.9
$p \to e^+\eta^\circ$	750-1100	< 0.3	0		0.37	0.54	0	0.2	
	400-650	< 0.5	1		0.07	0.15	0	2	12.
$p \to e^+\rho^\circ$	200-600	0.1-0.5	1		0.16	0.30	i	4	2.5
$p \to e^+\omega^\circ$	300-600	0.1-0.5	1		0.19	0.39	i	3	
	750-1100	< 0.3	0		0.05	0.06	0	0.2	4.0
$p \to \mu^+\gamma$	550-900	< 0.5	1	2	0.52	0.52	0	0.4	14.
$p \to \mu^+\pi^\circ$	550-900	< 0.4	1	1	0.32	0.44	b	0.2	5.1
$p \to \mu^+K^\circ$	150-400	0.1-0.5	1,2		0.19	0.20	f,i	2	
	550-900	<0.5	1		0.14	0.14	a,b	2	2.9
$p \to \mu^+\eta^\circ$	550-900	< 0.5	1		0.23	0.44	a,b	2	
	200-400	< 0.5	1,2		0.12	0.22	f,i	2	3.1
$p \to \mu^+\rho^\circ$	150-400	0.1-0.5	1,2		0.10	0.16	f,i	2	1.2
$p \to \mu^+\omega^\circ$	200-450	0.1-0.5	1,2		0.18	0.32	f,i	2	
	650-900	< 0.5	1		0.03	0.05	a,b	0.8	2.1
$p \to \nu K^+$	150-375	0.3-0.6	1		0.08	0.08	3	4	0.7
$p \to \nu \rho^+$	300-600	0.2-0.5	1		0.07	0.19	1	3	1.1
$p \to \nu K^{*+}$	250-500	0.3-0.6	1		0.09	0.19	4	4	0.7
$p \to e^+e^+e^-$	750-1100	< 0.3	0		0.93	0.93	0	0.2	25.
$p \to \mu^+\mu^+\mu^-$	200-425	< 0.5	2,3		0.58	0.58	f	0.2	9.
$n \to e^+\pi^-$	450-950	< 0.5	0		0.40	0.55	c,e,g,h	4	2.5
$n \to e^-\pi^+$	400-700	< 0.5	1		0.10	0.24	0	2	
	700-950	< 0.5	0		0.10	0.07	c,e	2	2.5
$n \to e^+\rho^-$	400-800	< 0.4	0		0.20	0.42	c,d,e,g	2	1.2
$n \to e^-\rho^+$	400-800	< 0.4	0,1		0.22	0.57	a,c,d,e,g	3	1.2
$n \to \mu^+\pi^-$	200-700	< 0.5	1		0.30	0.43	i	4	3.8
$n \to \mu^-\pi^+$	200-500	< 0.5	1,2		0.29	0.45	f,i	3	2.7
$n \to \mu^+\rho^-$	300-550	< 0.5	1		0.07	0.29	i	2	0.9
$n \to \mu^-\rho^+$	300-550	< 0.5	1,2		0.10	0.41	f,i	2	0.9
$n \to \nu\gamma$	350-600	0.5 <	0		0.77	0.77	28	19	1.1
$n \to \nu\pi^\circ$	350-600	0.5 <	0		0.51	0.82	28	19	0.7
$n \to \nu K^\circ$	450-700	0.2-0.5	0		0.10	0.11	2	2	1.0
$n \to \nu\eta^\circ$	450-800	0.1-0.5	0		0.29	0.56	4	3	1.8
$n \to \nu\rho^\circ$	150-500	0.1-0.4	0,1		0.05	0.11	7	3	0.2
$n \to \nu\omega^\circ$	200-450	0.2-0.5	1		0.08	0.24	1	2	
	650-950	< 0.3	0		0.03	0.06	0	0.3	1.6
$n \to \nu K^{*\circ}$	200-700	.15-0.5	1		0.06	0.11	1	4	0.7
$n \to e^+e^-\nu$	500-850	< 0.5	0		0.41	0.41	4	3	2.6
$n \to \mu^+\mu^-\nu$	150-375	0.2-.65	1,2		0.31	0.31	4	7	1.9

See next page for column number notes.

Notes to column numbers in Table III:

1. For 3-body decay modes flat phase space was assumed.
2-4. Different requirement regions correspond to different meson decay modes.
4. Number of muon decay signals required.
5. Number of events rejected by requiring two clear tracks with opening angle >140°. Columns 6 and 7 include a 90% scanning efficiency for this requirement.
8. Some events are candidates for more than one mode. The letters a through i represent the candidate events listed in Table IV.
9. Background estimates for the scanned modes have a rejection factor of 75% evaluated by scanning of simulated events. (See Col. 5.)
10. Lifetime limits quoted are at 90% C.L. for 204 live days and do not include background subtraction.
† K°_{L} decays are included.

Table IV - Events Passing All the Requirements for Non-ν Modes

	Event No.	E_c (MeV)	Anisotropy A	No. of μ Decay
a	143-21939	745	0.40	1
b	225-7794	880	0.27	1
c	299-72044	735	0.33	0
d	420-34248	425	0.11	0
e	510-54208	720	0.36	0
f	588-8320	385	0.50	2
g	656-11673	510	0.37	0
h	663-1770	560	0.41	0
i	747-44203	340	0.45	1

determined from a 5 year ν simulation. Figure 5(b) above shows the E_c vs. A plot for simulated neutrino interaction which is normalized to 204 days of detector livetime.

Table III summarizes the cuts and results for the 32 nucleon decay modes. Refer to the "notes" for an explanation of the various numbered columns. The nucleon lifetime limits are 90% C.L. level limits obtained without a background subtraction. These limits may be improved when the background estimates are better understood. For nucleon decay modes which do not include a neutrino, there are 9 data events which fall within the union of all cuts. These 9 events are listed in Table IV. Many of these events are consistent with more than one decay mode. The labels "a" through "i" in the table are used to cross reference column 8 in Table III which lists the events which are consistent with the cuts of the various modes.

CONCLUSION

In summary, the IMB experiment has obtained the following results:

- No Monopole catalysis of nucleon decay events have been observed yielding a measured 90% C.L. upper limit on the monopole flux of

$$F_m < 2.1 \times 10^{-15} \text{ cm}^{-2} \text{ sr}^{-1} \text{ s}^{-1}$$

for a catalysis interaction length $\lambda_C \leq 0.1$ m and for a monopole velocity in the range $10^{-3} < \beta_m < 10^{-1}$.

- The search for $n \to \bar{n}$ transitions in oxygen nuclei has produced 3 events consistent with neutrino induced background. No background subtraction is made and a 90% C.L. lower limit is obtained for the bound lifetime

$$\text{(bound)} \quad \tau (n \to \bar{n}) > 2.4 \times 10^{31} \text{ yrs.}$$

using the calculation of Dover et al., this translates into a lower limit on the free-neutron oscillation time

$$\text{(free)} \quad \tau (n \to \bar{n}) > 8.8 \times 10^{7} \text{ seconds.}$$

- In 204 days of analyzed data, 169 events have been observed which are fully contained within the detector fiducial volume. These are used to set limits on 32 nucleon decay modes which are reported in Table III. The overall rate of the events are consistent with neutrino interactions. However, there are 9 events listed in Table IV which are also consistent with nucleon decay into various modes. In general, there is no evidence for nucleon decay at the level of $\sim 10^{32}$ years for 2-body modes like $e^+\pi^\circ$, $\mu^+\pi^\circ$, $e^+\eta^\circ$, $\mu^+\eta^\circ$, etc. For more complicated modes involving K's, K*'s, or ν's, there is no evidence for nucleon decay at the level of a few $\times 10^{31}$ years.

ACKNOWLEDGEMENTS

We wish to thank the many people who helped bring the IMB detector into successful operation. We are particularly grateful to our host, Morton-Thiokol Inc., who operate the Fairport Harbor Mine. One of us (JLS) expresses special thanks and appreciation to all of the Bielefeld organizers, especially R. Baier, for hosting this informative and very successful conference.

REFERENCES

1. C.G. Callan Jr., Phys. Rev. D 26, 2058 (1982) and 25, 2141 (1982).
2. V.A. Rubakov, Nucl. Phys. B203, 311 (1982), and Pis'ma Zh. Eksp. Teor. Fiz. 33, 658 (1981) [JETP Lett.33, 644 (1981)].
3. F. Wilczek, Phys. Rev. Lett 48, 1146 (1982).
4. M.R. Krishnaswami et al., Proceedings of the 18th International Cosmic Ray Conference (Bangalore), 7, 95 (1983).
5. J. Bartelt et al., Phys. Rev. Lett. 50, 651 and 655 (1983).
6. G. Battistoni et al., Phys. Lett. 118B, 461 (1982).
7. M. Koshiba, private communication.
8. S. Errede et al., Phys. Rev. Lett 51, 245 (1983); R.M. Bionta et al., Phys. Rev. Lett 51, 27 (1983).
9. S.M. Errede, Monopole '83, edited by J.L. Stone (Plenum Publishing Corp., New York, 1984).

10. R.N. Mohapatra, Proceedings of the Informal Workshop on Neutron-Antineutron Oscillations, edited by M.S. Goodman, M. Machacek, and P.D. Miller (Harvard University, Cambridge, 1982).
11. T.W. Jones et al., Phys. Rev. Lett. 52, 720 (1984).
12. C.B. Dover, A. Gal, and F.M. Richard, Phys. Rev. D27, 1090 (1983).
13. H.S. Park et al., submitted to Phys. Rev. Lett. October 1984.